PCCP

Cite this: *Phys. Chem. Chem. Phys.*, 2012, **14**, 15525–15538

www.rsc.org/pccp

PAPER

How membrane permeation is affected by donor delivery solvent†

Bernard P. Binks,[a] Paul D. I. Fletcher,*[a] Andrew J. Johnson[a] and Russell P. Elliott[b]

Received 6th August 2012, Accepted 4th October 2012
DOI: 10.1039/c2cp42747h

We investigate theoretically and experimentally how the rate and extent of membrane permeation is affected by switching the donor delivery solvent from water to squalane for different permeants and membranes. In a model based on rate-limiting membrane diffusion, we derive explicit equations showing how the permeation extent and rate depend mainly on the membrane-donor and membrane-receiver partition coefficients of the permeant. Permeation results for systems containing all combinations of hydrophilic or hydrophobic donor solvents (aqueous solution or squalane), permeants (caffeine or testosterone) and polymer membranes (cellulose or polydimethylsiloxane) have been measured using a cell with stirred donor and re-circulating receiver compartments and continuous monitoring of the permeant concentration in the receiver phase. Relevant partition coefficients are also determined. Quantitative comparison of model and experimental results for the widely-differing permeation systems successfully enables the systematic elucidation of all possible donor solvent effects in membrane permeation. For the experimental conditions used here, most of the permeation systems are in agreement with the model, demonstrating that the model assumptions are valid. In these cases, the dominant donor solvent effects arise from changes in the relative affinities of the permeant for the donor and receiver solvents and the membrane and are quantitatively predicted using the separately measured partition coefficients. We also show how additional donor solvent effects can arise when switching the donor solvent causes one or more of the model assumptions to be invalid. These effects include a change in rate-limiting step, permeant solution non-ideality and others.

Introduction

Permeation of a species from a donor to a receiver compartment across a membrane is important in many applications, including retention of perfumes and flavours within food packaging, exclusion of toxic chemicals by chemical safety suits, control of pests and plant diseases using bioactive agrochemicals, cosmetics and delivery of pharmaceutical actives across membrane barriers such as the skin. The permeating species may be contacted with the donor side of the membrane in a variety of formulation types (or "vehicles") including, *inter alia,* solutions in either water or low polarity organic solvents. For pharmaceutically-relevant applications, the receiver compartment commonly contains an aqueous solution of electrolytes, designed to mimic blood serum. The aim of this work is to understand how changing the donor compartment solvent can affect the rate and extent of membrane permeation to a receiver compartment containing an aqueous electrolyte solution. We seek to elucidate (i) all possible origins of these donor solvent effects; (ii) how to resolve which effect or effects may be operating in a particular system and (iii) how the donor solvent effects depend on the natures of both the permeating species and the membrane.

There is an extensive literature on membrane permeation covering both biological membranes such as skin and synthetic, polymer membranes. Effects of donor solvent type, including both thermodynamic (reflecting the relative affinity of the permeant for the membrane) and kinetic effects (how solvent type affects the diffusivity of the permeant in the membrane) have been investigated.[1–6] Donor vehicles have included not only single-solvent solutions but also permeants dissolved in mixed solvents[7–12] and more complex, multi-phase vehicles such as emulsions; including oil-in-water, water-in-oil and multiple types stabilised by either surfactants, polymers or particles.[13–22] Overall, it is well established that the extent and rate of permeation for a particular permeating species and membrane system depends strongly on the nature of the liquid formulation vehicle applied to the donor side of the membrane. As discussed later, donor solvent effects can arise

[a] *Surfactant & Colloid Group, Department of Chemistry, University of Hull, Hull, HU6 7RX, UK. E-mail: P.D.Fletcher@hull.ac.uk; Fax: +44 (0)1482 466410; Tel: +44 (0)1482 465433*
[b] *Stiefel, a GSK Company, 20 TW Alexander Drive, Research Triangle Park, NC 27709, USA*

† Electronic supplementary information (ESI) available. See DOI: 10.1039/c2cp42747h

from many possible causes which can depend on both the nature of the specific system together with details of the experimental conditions (for example, donor and receiver compartment stirring rates, volumes and membrane thicknesses) used in the permeation measurements. Despite numerous literature reports of donor solvent effects on permeation, many of the studies lack sufficient detailed information to enable unambiguous resolution of which effect or combination of effects may be operating in particular donor vehicle systems. An additional problem is that switching between the same polar and apolar donor solvents can affect permeation in dramatically different ways for systems with different permeating species or membranes. Hence, although many individual aspects of donor solvent effects on permeation have been reported, there remains a clear need to clarify (i) all the possible origins of such effects and how to discriminate between them and (ii) how donor solvent effects depend on the natures of the permeant and the membrane. The aim of this work is to address both these points using a combination of theory and experiment.

We tackle the overall problem in several steps. Firstly, we develop a theoretical model based on the assumption that the rate-determining step of the overall mass transport of the permeant from donor to receiver compartments is diffusion across the membrane, *i.e.* that all other steps in the overall process, such as diffusion within the donor or receiver compartment solutions and entry or exit of the membrane are relatively fast. This theory enables quantitative prediction of how the donor solvent affects both the extent and rate of permeation for all combinations of permeant and membrane species for systems and conditions for which the set of model assumptions are valid. Secondly, we measure the permeation kinetics for all combinations of hydrophilic and hydrophobic donor solvents (aqueous solution and squalane), hydrophilic and hydrophobic permeants (caffeine and testosterone) and hydrophilic and hydrophobic membranes (cellulose and polydimethylsiloxane, PDMS). Thirdly, using ancillary measurements of partition coefficients, the experimental permeation rate data are compared with the predictions of the theoretical model. The model comparisons enable us to distinguish between experimental systems which obey the model assumptions and those which do not. In turn, this enables a rigorous resolution of which of the different possible donor solvent effects are operating in the different experimental systems.

This paper is organised as follows. Experimental details are given in the Materials and Methods section. In the Results section, we first develop the theoretical framework and summarise how the donor solvent is expected to affect the rate and extent of membrane permeation for systems for which the relevant assumptions are valid. Secondly, experimental results are presented for the partition coefficients of the different systems, measured as a function of the permeant concentrations to assess the extent to which ideal permeant solution behaviour is followed. We then present examples of permeation rate measurements in the form of plots of receiver compartment concentration *versus* time from which experimental values of the permeation rate coefficient k and the equilibrium receiver compartment concentration $C_{\mathrm{rec},\infty}$ are derived. We show examples of systems which follow the behaviour predicted by the theoretical model and data for systems which show deviations. The experimental values of k and $C_{\mathrm{rec},\infty}$ for all the different systems are compared with values predicted using the theoretical model. In the Discussion section, all possible types of donor solvent effects are discussed, including those which operate in systems for which the model assumptions are valid and the effects which arise when the different model assumptions are invalid. Finally, the key conclusions, significance and applicability of the results are summarised in the Conclusions section.

Materials and methods

Materials

Water was purified by passing through an Elgastat Prima reverse osmosis unit followed by a Millipore Milli-Q reagent water system. The resistivity and air–water surface tension at 25 °C were 16 MΩ cm and 71.9 mN m^{-1} respectively. The pH was 6.5. Squalane (>99% purity, Sigma-Aldrich) was passed through a column of acidic alumina (Merck) in order to remove polar impurities. Phosphate buffered saline (PBS) solution, containing 137 mM NaCl, 2.7 mM KCl, 10 mM Na_2HPO_4 and 2 mM KH_2PO_4, had a pH of 7.3. Inorganic salts used to prepare the PBS (NaCl, BDH, >99.5%; KCl, BDH, >99.5%; Na_2HPO_4, Fischer Scientific, >99% and KH_2PO_4, BDH, >99%) were used as supplied. Testosterone (TCI Europa, Belgium, 98%) and caffeine (>99%, Sigma-Aldrich) were used as received.

Polydimethylsiloxane (PDMS) elastomeric membranes (model 7-4107) were a gift from Dow Corning, Europe and had a mean thickness of 81 ± 15 μm. Cellulose membranes were dialysis membranes (12–14 kD molecular weight cut-off, Medicell International Ltd.) and had a dry membrane thickness of 23 μm. They were pre-soaked in PBS for 24 hours prior to use. The membranes were cut to size with a clean, sharp scalpel and washed repeatedly with PBS solution. Following soaking experiments for 24 hours, it was found that the PDMS membrane did not swell significantly in PBS or squalane in either area or thickness. The cellulose membrane was not swollen by the squalane; however, soaking in PBS caused no change in membrane area but did cause the thickness to increase from 23 to 48 μm.

Partition coefficient measurements

The equilibrium partition coefficients of caffeine and testosterone between aqueous PBS and squalane were measured by contacting a known volume (typically 5.0 ml) of permeant solution of the required concentration in aqueous PBS (for caffeine) or squalane (for testosterone) with a known volume of the appropriate second phase. The mixture was stirred at 1000 rpm at 32 °C for either 1 or 2 weeks in a sealed vessel. Following this equilibration, the organic and aqueous layers were allowed to separate, samples of both phases were withdrawn and the equilibrium permeant concentration determined by UV-vis spectrophotometry. Calibration plots of UV absorbance *versus* concentration for the different permeants and solvents are shown in the ESI.† Control

measurements were made using samples with no permeant in order to correct the measured UV absorbance values for small (typically 10% or less) errors due to the presence of trace UV absorbing impurities arising from the squalane. The concentration values enabled the calculation of the partition coefficient K, equal to the ratio of equilibrium permeant concentrations in the two phases. It was found that either 1 or 2 weeks equilibration time yielded identical K values. The solubilities of testosterone and caffeine in both PBS and squalane were measured by equilibrating excess solid with the solvent followed by phase separation and analysis using UV-vis spectrophotometry.

The equilibrium partition coefficients of the permeants (caffeine and testosterone) between either aqueous PBS or squalane and the two membranes (PDMS and cellulose) were measured by equilibration of known volume of permeant solution of known initial concentration with a known volume of the membrane at 32 °C. Following equilibration, the equilibrium permeant concentration in the solution phase (decreased by loss of permeant to the membrane) was determined spectrophotometrically and the result used to calculate K. The value of K measured in this way did not change with equilibration times varying from 1 day to 5 weeks. Each final value of K was the mean of 5 independent measurements. Control measurements with systems containing no permeant were again used to correct UV absorbance values for trace UV-absorbing impurities leached from the membranes. This correction was less than 5% in all cases.

Membrane permeation measurements

Permeation rates from a donor compartment through a membrane to a flow-through receiver compartment were measured using a #1K001-15-VD permeation cell supplied by PermeGear. This cell has a circular membrane window (diameter 15 mm, exposed membrane area 1.76 cm^2) and an upper, fixed volume (2.18 ml) donor compartment which is sealable with a screw-cap septum. The cell, constructed from chemically inert polychlorotrifluoroethylene (PCTFE), was thermostatted at 32 °C and the donor compartment was magnetically stirred with a stirrer bar of 12.5 × 3.5 mm rotating at 5000 rpm (except where noted otherwise). The receiver compartment solution had a fixed total volume of 3.17 ml and was pumped continuously at 3 ml min^{-1} through a flow-through quartz cuvette with a 10 mm path length, mounted within a temperature controlled Unicam UV3 UV-vis Spectrophotometer also maintained at 32 °C. Receiver solution UV-absorbance values were captured and logged at 20 s intervals over permeation runs lasting up to 40 hours. The receiver solution was pumped using a Spectra System P1500 Isocratic Liquid Chromatography Pump with a dual sapphire piston mechanism to produce a pulse-free flow. All solution absorbance values, measured at the appropriate wavelength corresponding to the maximum optical adsorbance of the permeant (251 nm for testosterone in PBS and 273 nm for caffeine in PBS), were converted to concentrations using the linear Beer–Lambert calibration plots shown in the ESI.†

All measurements were made at 32.0 ± 0.5 °C.

Results

Theory

We consider the permeation from a stirred solution in the donor compartment, through a membrane to a receiver solution of fixed volume which is recirculating. In order to establish a basic theoretical framework, the following assumptions are made. The validity or otherwise of these assumptions for particular experimental conditions must, of course, be questioned and tested for all comparison with experiments. Firstly, the rate limiting step is assumed to be diffusion of the permeating species across the membrane, *i.e.* all mass transfer and partitioning steps within the bulk donor and receiver compartments and transfer across the solution–membrane interfaces are relatively fast. Secondly, the lag time required to establish a steady-state mass transfer rate is negligibly small compared with the overall timescale of the permeation. Thirdly, we assume the diffusion of the permeant in the membrane follows Fick's Laws, that the membrane is uniform and that the diffusion coefficient has a fixed value which is independent of the permeant concentration in the membrane. Fourthly, it is assumed that only the single permeant species permeates across the membrane, *i.e.* the donor and receiver compartment solvents do not cross the membrane. If solvent permeation occurs, this would cause changes in the partition coefficients of the permeant as a function of time as the donor and receiver phase compositions change. Finally, the theory is restricted to uncharged permeant species and we assume that the permeant solutions in the donor, receiver and membrane volumes behave ideally, *i.e.* that concentrations can be substituted for activities in equations for equilibrium partition coefficients.

For the experimental permeation measurements described below, a permeant solution of initial concentration $C_{don,0}$ is loaded into the donor compartment and the permeant concentration C_{rec} in the fixed-volume, recirculating receiver compartment is recorded over time, from its initial value of zero until the final, equilibrium value $C_{rec,\infty}$ is reached. To fit the experimental permeation runs, we derive an analytical expression for the variation of C_{rec} with time t as follows. With the first assumption listed above, the local permeant concentrations in the membrane on the donor and receiver sides ($C_{mem,d}$ and $C_{mem,r}$) are maintained in local equilibrium with the concentrations C_{don} and C_{rec} and hence:

$$C_{mem,d} = K_{mem-don}C_{don} \quad (1)$$

$$C_{mem,r} = K_{mem-rec}C_{rec} \quad (2)$$

The ratio of donor and receiver concentrations ($=C_{don}/C_{rec}$) is not maintained equal to the equilibrium partition coefficient $K_{don-rec}$ during a permeation run; the equilibrium value is only reached at long times when C_{don} and C_{rec} achieve their equilibrium values of $C_{don,\infty}$ and $C_{rec,\infty}$. For the purposes of this derivation, all partition coefficients are denoted using the consistent nomenclature that $K_{a-b} = C_a/C_b$ where K_{a-b} is the partition coefficient of permeant between phases a and b and C_a and C_b are the equilibrium permeant concentrations in phases a and b respectively.

For permeation times longer than the so-called "lag-time", Fick's second law predicts that a linear concentration gradient of permeant across the membrane is established and permeation under these conditions is denoted as "steady-state". The steady-state permeant concentration gradient across the membrane (dC_{mem}/dx) is:

$$\frac{dC_{mem}}{dx} = \frac{(C_{mem,d} - C_{mem,r})}{X} \quad (3)$$

where C_{mem} is the permeant concentration at depth x in the membrane and X is the total membrane thickness. The rate of change of permeant concentration in the receiver compartment (dC_{rec}/dt) is related to the concentration gradient across the membrane according to Fick's first law:

$$\begin{aligned}\frac{dC_{rec}}{dt} &= \left(\frac{AD}{XV_{rec}}\right)(C_{mem,d} - C_{mem,r}) \\ &= \left(\frac{AD}{XV_{rec}}\right)(K_{mem-don}C_{don} - K_{mem-rec}C_{rec})\end{aligned} \quad (4)$$

where A is the surface area of the membrane, D is the diffusion coefficient of the permeant in the membrane and V_{rec} is the volume of the receiver compartment. At any time during the permeation, the total amount of permeant in the whole system is distributed between the donor and receiver compartments and the membrane and consideration of the permeant mass balance gives:

$$C_{don} = \frac{(n_t - C_{rec}V_{rec} - C_{mem}V_{mem})}{V_{don}} \quad (5)$$

where n_t is the total number of moles of permeant, V_{don} and V_{mem} are the volumes of the donor compartment and membrane and C_{mem} is the average concentration of permeant within the membrane. Under steady-state permeation conditions, the permeant concentration in the membrane varies linearly between $C_{mem,d}$ and $C_{mem,r}$ and hence $C_{mem} = (C_{mem,d} + C_{mem,r})/2$. Substituting for C_{mem} according to eqn (1) and (2) gives, after some re-arrangement, the following expression for C_{don} in terms of C_{rec}.

$$\begin{aligned}C_{don} = &\frac{n_t/V_{don}}{(1 + (K_{mem-don}V_{mem}/2V_{don}))} \\ &- \frac{(V_{rec}/V_{don} + K_{mem-rec}V_{mem}/2V_{don})}{(1 + (K_{mem-don}V_{mem}/2V_{don}))}C_{rec}\end{aligned} \quad (6)$$

Eqn (6) can be expressed in the form $C_{don} = Y - ZC_{rec}$ where Y is the first term in eqn (6) and Z, is the multiplier term of C_{rec}. Substituting this expression for C_{don} into eqn (4) yields:

$$\frac{dC_{rec}}{dt} = \left\{\frac{ADK_{mem-don}Y}{XV_{rec}}\right\} - \left\{\frac{AD(K_{mem-don}Z + K_{mem-rec})}{XV_{rec}}\right\}C_{rec} \quad (7)$$

Integration of this equation leads to:

$$C_{rec} = C_{rec,\infty} + (C_{rec,0} - C_{rec,\infty})\exp(-kt) \quad (8)$$

where $C_{rec,0}$ and $C_{rec,\infty}$ are the initial and the equilibrium values of the permeant concentration in the receiver compartment respectively. From eqn (8), it can be seen that C_{rec} is predicted to increase exponentially from $C_{rec,0}$ to $C_{rec,\infty}$ with a first-order permeation rate coefficient k (units: s^{-1}). Experimental permeation plots of C_{rec} *versus* time are fully characterised by two parameters: $C_{rec,\infty}$ and k which, in turn, are given by:

$$C_{rec,\infty} = \left\{\frac{K_{mem-don}Y}{K_{mem-don}Z + K_{mem-rec}}\right\} \quad (9)$$

$$k = \left\{\frac{AD(K_{mem-don}Z + K_{mem-rec})}{XV_{rec}}\right\} \quad (10)$$

The final equations reveal the key observable characteristics of experimental permeating systems for which the underpinning model assumptions are valid.

(1) The variation of C_{rec} with time is predicted to follow an exponential curve.

(2) The value of the 1st-order permeation rate coefficient k is predicted to be independent of the initial permeant concentration in the donor compartment.

(3) The values of $C_{rec,\infty}$ and k are predicted to be independent of donor stirring rate and receiver compartment flow-through rate as long as these are sufficiently high to ensure mass transport within either the donor or receiver compartments is not rate-determining.

(4) The values of $C_{rec,\infty}$ and k are predicted to depend on the nature of the permeant, donor and receiver solvents and the membrane as expressed by the values of membrane diffusion coefficient D and the two partition coefficients $K_{mem-don}$ and $K_{mem-rec}$.

(5) The values of $C_{rec,\infty}$ and k are predicted to depend on the geometrical parameters of the permeation system, *i.e.* A, V_{don}, V_{rec} and V_{mem}.

Eqn (8)–(10) enable the prediction of how the rate and extent of permeation from donor to receiver depend on the chemical natures of the permeant, the donor and receiver solvents and the membrane. For the purposes of this prediction, in order to remove factors such as permeant concentration and the geometrical parameters of the permeation system, we set $V_{don} = V_{rec}$ and $V_{mem} = 0$. The permeation rate is expressed as the dimensionless rate coefficient (kXV_{rec}/AD) and the extent of permeation as the fraction of total permeant which is extracted from the donor to the receiver compartment at equilibrium. The different combinations of hydrophilic/hydrophobic permeant, donor solvent and membrane can be represented in terms of hypothetical values of $K_{mem-don}$ and $K_{mem-rec}$ for each system as shown in Table 1. For this analysis, we have taken the partition coefficients to be either 40 (for a permeant partitioning from a low affinity environment to a high affinity environment, *e.g.* a hydrophobic permeant going from water to a hydrophobic membrane), 1 (for a permeant partitioning between two environments for which it has equal affinity) or 1/40 (for partitioning from a high affinity environment to a low one, *e.g.* for a hydrophilic permeant going from water to a hydrophobic membrane). Using these hypothetical K values with eqn (8)–(10) allows a simple means to visualise how the rate and extent of permeation are predicted to change with donor solvent for different permeant and membrane combinations. For the conditions

Table 1 Calculated values of fraction of total permeant extracted from donor compartment and dimensionless permeation rate coefficient for hypothetical systems containing all combinations of hydrophilic and hydrophobic donor solvents, permeants and membranes. Values have been designated as "high", "medium" or "low". The actual values used for the partition coefficients and derived for the fractions extracted and permeation rates are given in parentheses

Donor solvent	Permeant	Membrane	$K_{mem-don}$	$K_{mem-rec}$	Fraction permeant extracted	Dimensionless permeation rate coefficient (kXV_{rec}/AD)
Water	Hydrophobic	Hydrophobic	High (40)	High (40)	Medium (0.5)	High (80)
Oil	Hydrophobic	Hydrophobic	Medium (1)	High (40)	Low (0.024)	High (41)
Water	Hydrophilic	Hydrophobic	Low (0.025)	Low (0.025)	Medium (0.5)	Low (0.05)
Oil	Hydrophilic	Hydrophobic	Medium (1)	Low (0.025)	High (0.98)	Medium (1)
Water	Hydrophobic	Hydrophilic	Medium (1)	Medium (1)	Medium (0.5)	Medium (2)
Oil	Hydrophobic	Hydrophilic	Low (0.025)	Medium (1)	Low (0.024)	Medium (1)
Water	Hydrophilic	Hydrophilic	Medium (1)	Medium (1)	Medium (0.5)	Medium (2)
Oil	Hydrophilic	Hydrophilic	High (40)	Medium (1)	High (0.98)	High (41)

set here (*i.e.* $V_{don} = V_{rec}$ and $V_{mem} = 0$), the factor Z (see eqn (6)) reduces to 1, the factor Y reduces to $C_{don,0}$ and, from eqn (9), the fraction of permeant extracted $C_{rec,\infty}/C_{don,0}$ is equal to:

$$\frac{C_{rec,\infty}}{C_{don,0}} = \left\{\frac{K_{mem-don}}{K_{mem-don} + K_{mem-rec}}\right\} \quad (11)$$

Similarly, from eqn (10), the dimensionless permeation rate coefficient reduces to:

$$\frac{kXV_{rec}}{AD} = K_{mem-don} + K_{mem-rec} \quad (12)$$

As seen in Table 1, the calculated dimensionless permeation rate coefficients all lie within one of three ranges: high (41–80 for the K values taken here), medium (1–2) or low (0.05). The values of the equilibrium fraction of permeant extracted are similarly either high (0.98), medium (0.5) or low (0.024) depending on the ratio of $K_{mem-don}$ and $K_{mem-rec}$ which is equal to the overall partition coefficient $K_{rec-don}$. Although the values of $K_{mem-don}$ and $K_{mem-rec}$ used here (either 40, 1 or 1/40) are, of course, only broadly representative of the relative hydrophilic/hydrophobic natures of different permeant, donor solvent and membrane systems, the comparison of Table 1 allows useful insight into how widely differing systems are expected to permeate. Some of the results summarised in Table 1 follow easily from intuitive considerations of the relative affinities of the permeant for the donor and receiver solvents and the membrane. However, a key general, and less intuitive, conclusion is that the permeation rate coefficient is proportional to the *sum* of the two partition coefficients ($K_{mem-don} + K_{mem-rec}$), as seen in eqn (12). It is this relationship which causes the permeation rate effects of switching between the same polar and apolar donor solvents to vary widely between different permeant/membrane combinations.

The development of the theoretical framework based on the stated model assumptions enables the prediction and comparison of different, hypothetical system behaviour shown in Table 1. In the next step, we seek to determine (i) whether or not different real permeation systems obey the model predictions and (ii) how the rates and extents of permeation vary for widely differing systems. To this end, we have experimentally investigated the permeation of systems containing all possible combinations of permeant (testosterone (hydrophobic) or caffeine (hydrophilic)), donor solvent (PBS (hydrophilic) or squalane (hydrophobic)) and membrane (PDMS (hydrophobic) or cellulose (hydrophilic)). For each system, the receiver phase was PBS. Analysis of the experimental permeation behaviour in terms of the model requires knowledge of the partition coefficients relevant to each system; this is presented in the following section.

Permeant partition coefficients

Fitting the plots of experimental measurements of C_{rec} as a function of time yields values of the rate coefficient k and $C_{rec,\infty}$. Using eqn (9) and (10) to interpret these values requires knowledge of the two partition coefficients $K_{mem-don}$ and $K_{mem-rec}$ for each different permeant–solvent–membrane system. Two aspects require some additional discussion here. Firstly, as explained in the Methods section above, the membrane partition coefficients are measured by equilibrating permeant solution of known volume and initial concentration with a known membrane volume and deriving K from the measured depletion of permeant from the solution to the membrane. However, this method is not accurate if the magnitude of K is such that there is no significant depletion of the solution concentration by partitioning to the membrane. In these cases, the unknown value of K can be derived from measured values of two related partition coefficients. For example, $K_{PDMS-PBS}$ for caffeine is not directly measureable since too small a fraction of the caffeine distributes to the membrane to produce a measureable depletion of the PBS solution, even when the membrane : solution volume ratio is maximised. However, the value of $K_{PDMS-PBS}$ can be calculated using measured values of $K_{PBS-squalane}$ and $K_{PDMS-squalane}$, as shown below.

$$K_{PDMS-PBS} = \frac{C_{PDMS}}{C_{PBS}} = \frac{C_{PDMS}}{C_{squalane}}\frac{C_{squalane}}{C_{PBS}} = \frac{K_{PDMS-squalane}}{K_{PBS-squalane}} \quad (13)$$

Similar calculations are used to derive all partition coefficients which are not directly measureable. The second aspect to be considered is the effect of possible non-ideal solution behaviour on the partition coefficients. The true, concentration-independent value of a partition coefficient K_{a-b} is the equilibrium ratio of the solute *activity* in each phase ($=a_a/a_b$). The activities are then equal to the product of the activity coefficient γ and the concentration as shown below.

$$K_{a-b} = \frac{a_a}{a_a} = \frac{\gamma_a C_a}{\gamma_b C_b} \quad (14)$$

Hence, in general, an apparent K value (taken to equal the ratio of concentrations) will only equal the true value in the limit of low concentrations when the solutions in both phases behave ideally, which is when the activity coefficients reduce to unity. For finite concentrations, non-ideal behaviour in one or both of the phases is manifested as a concentration dependence of the apparent K value equal to the ratio of equilibrium concentrations.

Because of the two aspects noted above, apparent K values (equal to the ratio of equilibrium concentrations) have been measured for solvent–solvent combinations to enable the derivation of values for membrane–solvent combinations which are not directly measureable. In addition, all K values have been measured for different permeant concentrations in order to assess possible non-ideality effects. Fig. 1 shows plots of measured apparent K values *versus* the equilibrium concentration of the distributing species for all combinations of permeant, solvent and membrane used here. In each plot, the horizontal dashed line indicates the concentration range used in the permeation rate measurements since we are interested in the value of K which corresponds to that concentration range. In the upper plot, it can be seen that $K_{\mathrm{PBS-squalane}}$ for both caffeine and testosterone are concentration-independent over the concentration range relevant to the permeation rate measurements and hence average values over this concentration range are used. Slight non-ideality deviations from these low-concentration-range average values are observed at higher concentrations which continue up to the highest possible concentrations, equal to relevant solubilities. At 32 °C, the equilibrium solubilities of testosterone in water, PBS and squalane were measured to be 0.12, 0.098 and 0.81 mM respectively; the values for caffeine in water, PBS and squalane were 140, 122 and 0.48 mM respectively. Literature values for the solubilities in water for testosterone (0.11 mM at 31 °C and 0.13 mM at 35 °C) and for caffeine (133 mM at 30 °C and 167 mM at 35 °C) are in reasonable agreement.[23] The K values derived from the solubility ratio (marked by the vertical dashed lines) are in line with the trends of the plots. It is noted here that the use of K values derived from solubility ratios is not recommended since such values refer to the highest achievable concentrations and therefore are likely to be subject to errors due to non-ideal behaviour.

The middle graph of Fig. 1 shows plots for four different permeant–membrane–solvent systems for which apparent K values do not show significant variation with concentration, relative to the (fairly large) experimental uncertainties. In these cases, the average concentration-independent values of K used in the analysis of the permeation runs are indicated by the vertical axis positions of the horizontal dashed lines for each system. Finally, the lower graph of Fig. 1 shows the plot for caffeine distributing between the cellulose membrane and PBS where it can be seen that K varies significantly with caffeine concentration over the relevant concentration range.

The final values of all partition coefficients used in the analysis of the permeation rate measurements described below are summarised in Table 2. Where the entry is denoted as "concentration dependent", the value of K appropriate to the average concentration for each individual permeation rate run has been estimated using the fitting equation corresponding to the solid line of the lower plot of Fig. 1.

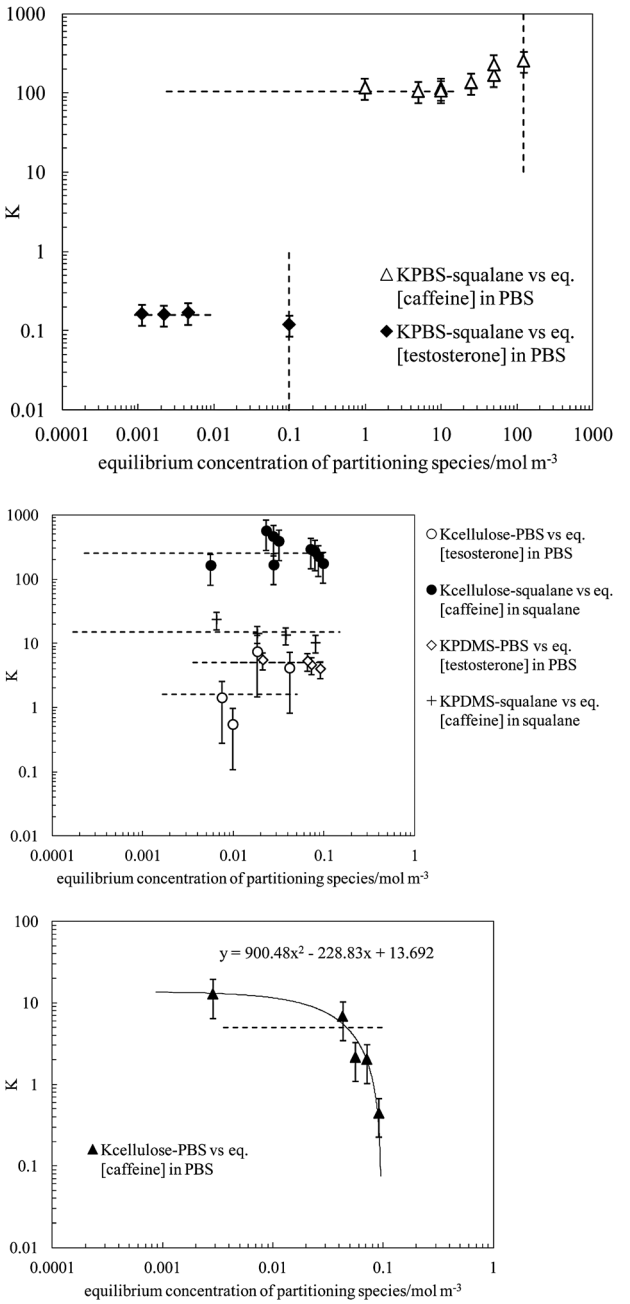

Fig. 1 Variation of measured partition coefficients at 32 °C with liquid phase concentration. For each plot the system details are indicated in the key and the horizontal dashed line indicates the concentration range used in the permeation experiments and the corresponding average value of K over the experimental concentration range. The upper plot for the PBS–squalane partition coefficients also includes vertical dashed lines which indicate the solubility values of the permeant for which K was taken to be the ratio of solvent solubilities. The lower plot, for caffeine partitioning between cellulose and PBS, shows K is concentration dependent over the relevant concentration range for this system.

Permeation rate measurements and their analysis

Fig. 2 shows examples of measured plots of C_{rec} *versus* time for caffeine permeating from a PBS donor phase with different initial concentrations of caffeine through a cellulose membrane to a PBS receiver phase. The observed behaviour of

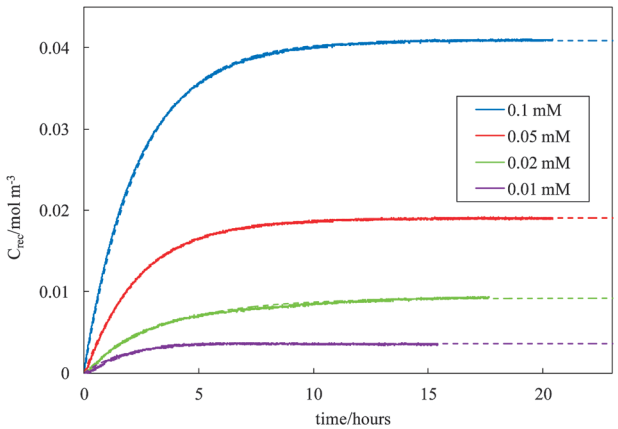

Fig. 2 Measured variation of receiver compartment concentration C_{rec} with time (solid lines) for caffeine in PBS permeating through cellulose at 32 °C. The initial donor compartment concentrations of caffeine (in descending order) are shown in the key; the dashed lines correspond to the best-fit to the exponential function predicted by theory (eqn (8)).

this system is accurately described by the theoretical model expressed through eqn (8)–(10). In particular, the measured curves are accurately exponential as expected from eqn (8); the rate coefficient k is virtually identical for all different initial donor phase concentrations and $C_{rec,\infty}$ scales with the initial donor phase concentration. Hence it is concluded that the set of assumptions underpinning the model are valid for this system under the experimental permeation conditions used here.

One of the model assumptions leading to the prediction of exponential concentration plots is that the permeation occurs under so-called steady-state conditions when the linear concentration gradient of permeant across the membrane is fully established. As detailed in ref. 24, the time required to establish this steady-state, (the so-called lag-time L) is given by the approximate expression below.

$$L \approx \frac{X^2}{6D} \qquad (15)$$

For the systems investigated here, the membrane thickness X ranges from 48 to 80 μm and (as discussed later) the values of permeant diffusion coefficient in the membrane D range from 1.6 to 16 × 10^{-12} m^2 s^{-1} (see Table 2). The values of L, estimated using eqn (15), for all the different systems measured here are listed in Table 2 and lie in the range from 24 to 683 s. All values of L are small relative to the timescales of the experimental permeation runs which are typically 5 to 50 hours and all the permeation runs occur under steady-state conditions for all but the first few minutes or so. Hence, for most of the systems, the plots of C_{rec} *versus* time are exponential in shape and do not show an obvious lag phase at short times. The estimated lag times are similar in magnitude to the experimental uncertainty in estimating time zero for permeation (approximately ±2 minutes), corresponding to the time required to load and seal the donor compartment of the permeation cell and initiate permeation. Lag time effects are discussed in more detail in the discussion section below.

From the theoretical discussion of permeation rates for the hypothetical permeant, donor solvent and membrane combinations summarised in Table 1, it is seen that the slowest permeation is predicted to occur for a combination of hydrophilic permeant from water as donor phase through a hydrophobic membrane. Of the different experimental systems measured here, this very slow permeation case is realised for caffeine permeating through a PDMS membrane from a PBS donor phase. Fig. 3 (upper plot) shows experimental plots of C_{rec} *versus* time for different initial concentrations of caffeine in the PBS donor phase. It can be seen that the permeation rate is so slow that the full exponential curves are not observed over the 15 hour timescales of the runs. The measured plots correspond to the permeation of only a small fraction of the total caffeine present and are approximately linear. The gradients of the lines correspond to the *initial* permeation rates which, according to the theoretical model, are predicted to scale with initial donor phase concentration with the constant of proportionality equal to the permeation rate coefficient k. The linear scaling of initial rate with initial concentration is shown in the lower plot of Fig. 3.

Of the eight combinations of permeant, donor solvent and membranes investigated experimentally, seven of the systems are observed to follow the theoretical model for the permeation conditions employed here. The system of caffeine permeating through a cellulose membrane from a squalane donor

Table 2 Equilibrium partition coefficients and permeant diffusion coefficients used to obtain the calculated values of $C_{rec,\infty}$ and k for all the measured combinations of hydrophilic and hydrophobic donor solvents, permeants and membranes at 32 °C. Estimated lag times L are also shown

Donor solvent	Permeant	Membrane	$K_{mem-don}$	$K_{mem-rec}$	$K_{rec-don}$	Permeant diffusion coefficient through membrane/m^2 s^{-1}	Lag time L/s
PBS	Testosterone (Hydrophobic)	PDMS (Hydrophobic)	5 ± 2	5 ± 2	1	9.3 × 10^{-12}[a]	118[c]
Squalane	Testosterone (Hydrophobic)	PDMS (Hydrophobic)	0.8[b]	5 ± 2	0.16 ± 0.05		
PBS	Caffeine (Hydrophilic)	PDMS (Hydrophobic)	0.14[b]	0.14[b]	1	1.6 × 10^{-12}[a]	683[c]
Squalane	Caffeine (Hydrophilic)	PDMS (Hydrophobic)	15 ± 5	0.14[b]	105 ± 30		
PBS	Testosterone (Hydrophobic)	Cellulose (Hydrophilic)	1.6 ± 1.3	1.6 ± 1.3	1	16 × 10^{-12}[a]	24[c]
Squalane	Testosterone (Hydrophobic)	Cellulose (Hydrophilic)	0.26[b]	1.6 ± 1.3	0.16 ± 0.05		
PBS	Caffeine (Hydrophilic)	Cellulose (Hydrophilic)	Conc. dep	Conc. dep	1	3.0 × 10^{-12}[a]	128[c]
Squalane	Caffeine (Hydrophilic)	Cellulose (Hydrophilic)	250 ± 130	Conc. dep	105 ± 30		

[a] Obtained by fitting measured permeation rates. [b] Derived from measured K values. [c] Lag times estimated using eqn (15).

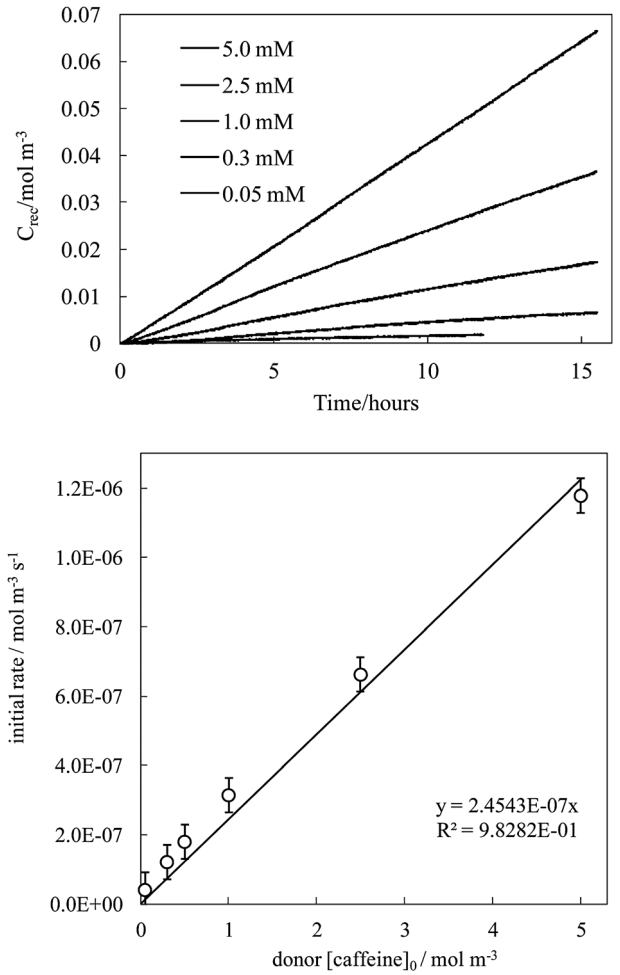

Fig. 3 Measured initial rate of change of receiver compartment concentration C_{rec} with time for caffeine permeating through PDMS from PBS donor solutions (upper plot) at 32 °C. The initial donor compartment concentrations of caffeine (in descending order) are shown in the key. The lower plot shows the derived variation of initial permeation rate *versus* initial donor concentration; the solid line shows the linear fit used to obtain k.

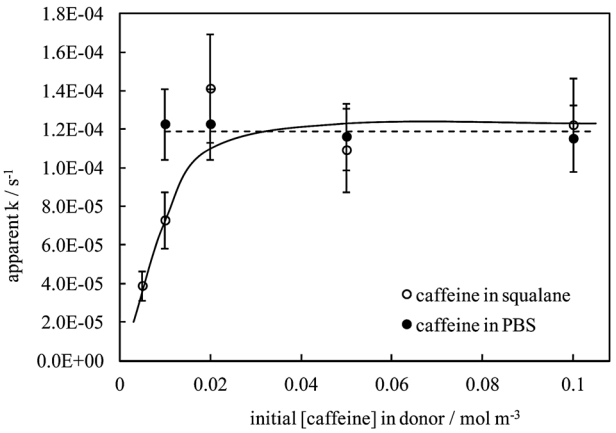

Fig. 4 Variation of apparent k value with initial caffeine concentration in the donor compartment for permeation of caffeine through cellulose from either PBS or squalane at constant donor stirring speed (using magnetic stirrer) of 4200 rpm. The horizontal dashed line corresponds to the "true" k value for caffeine in PBS, *i.e.* corresponding to membrane permeation being rate limiting for which k is independent of the initial concentration.

solution shows anomalous behaviour. In particular, the measured plots of C_{rec} *versus* time are observed to deviate from exponential behaviour and the permeation rate coefficient k is not independent of the initial donor phase concentration. Fig. 4 shows that k is independent of initial concentration for caffeine permeating through cellulose from PBS but dependent for squalane as the donor solvent. The caffeine–cellulose–squalane system was examined in further detail to determine which of the theoretical model assumptions may not be valid for this case. We first note that the permeant caffeine has a very high partition coefficient from the squalane donor solvent to the cellulose membrane ($K_{cellulose-squalane}$ = 250) and hence the permeation is predicted to be very rapid. Furthermore, squalane as donor solvent is approximately 26 times more viscous than PBS (20.8 mPa s compared with 0.76 mPa s[25]) which is expected to slow mass transport within the donor phase. Hence, it was hypothesised that the rate-limiting step of the overall permeation process may be switched from the membrane diffusion step (assumed in the model) to mass transport within the squalane donor phase. This hypothesis was tested by investigating how donor phase stirring speed affected the permeation, as shown in Fig. 5. If membrane diffusion is rate-limiting, the permeation rate coefficient k is expected to be unaffected by donor compartment stirring speed whereas increased stirring will increase the permeation rate if mass transport within the donor phase is rate limiting. Fig. 5 (upper plot) shows illustrative traces of C_{rec} *versus* time for two different stirring speeds in the squalane donor compartment. It can be seen that the curves deviate from exponential behaviour and that increased stirring speed increases the permeation rate. Fig. 5 (lower plot) shows that k derived from C_{rec} *versus* time plots is independent of stirring speed for caffeine permeating through cellulose from PBS but strongly dependent when permeating from a squalane donor solution. One permeation rate run was made with decane as the donor solvent because decane has a viscosity (0.78 mPa s[26]) much lower than squalane (20.8 mPa s) and similar to that of PBS (0.76 mPa s). If it is assumed that the affinity of the caffeine for decane and squalane are similar, then the k value observed for decane is expected to be similar to that predicted for squalane if mass transport in the donor phase were not rate-limiting. As seen in Fig. 5, the decane value and the highest stirring speed squalane measurement are reasonably similar. The conclusion here is that the anomalous behaviour of the caffeine–cellulose–squalane system is due to a switch in rate-limiting step to mass transport in the donor phase under the standard permeation conditions used here. For this system, rate-limiting membrane diffusion is only approached at the highest donor stirring speed used and k under these conditions is approximately 1×10^{-3} s^{-1}. Apparent k values measured at lower stirring speeds should not be analysed in terms of the theoretical model used here.

Following exclusion of the low donor stirring speed data for the caffeine–cellulose–squalane system, the experimental values of k and $C_{rec,\infty}$ for all systems were compared with

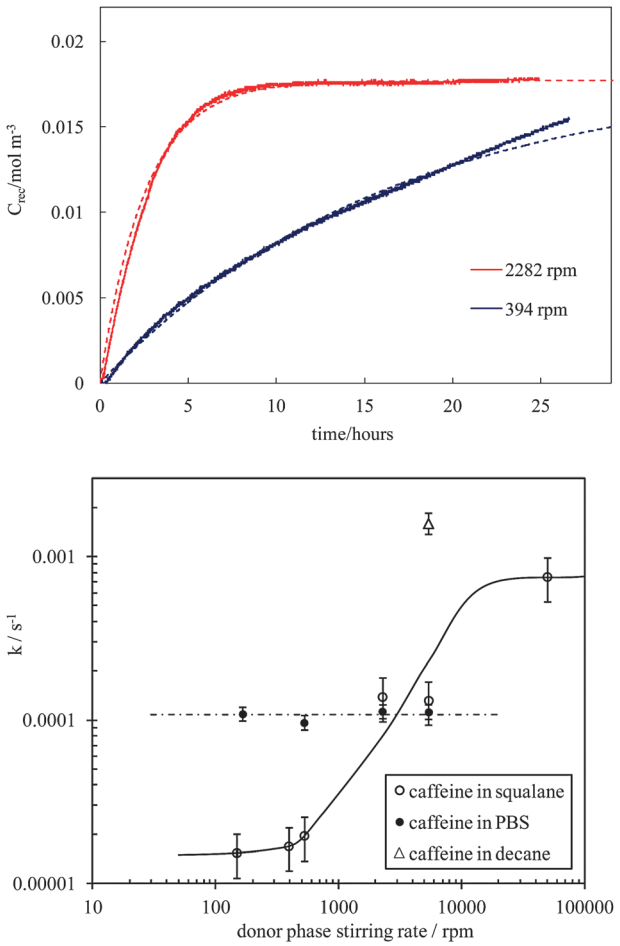

Fig. 5 Upper plot: Variation of C_{rec} *versus* time for permeation of caffeine through cellulose from identical squalane donor solutions for two different stirring speeds of the donor compartment. The dashed lines indicate the "best-fit" exponential curves. Lower plot: Variation of the apparent k value with donor stirring speed for permeation of caffeine through cellulose from either PBS or squalane donor solutions. A single value for decane as donor phase is also shown. The solid line is a guide for the eye. The horizontal dashed line corresponds to the stirring speed-independent k value for the PBS solution.

values calculated according to the theoretical model (eqn (8)–(10)). As discussed earlier and summarised in Table 2, all partition coefficients were measured or derived from measured values with proper consideration of solution non-ideality effects appropriate to the concentration ranges used. The diffusion coefficients D for the different permeant and membrane combinations were not measured directly; they were obtained by fitting measured and calculated k values using the solver function in Microsoft EXCEL. In this fitting procedure, it was assumed that D was not affected by the donor solvent used, *i.e.* D depended only on the nature of the permeant and the membrane. Hence, the eight different permeant–solvent–membrane systems yield four values of D which are summarised in Table 2. Some limited comparison of these D values with literature can be made as follows. D for testosterone in PDMS at 32 °C estimated here (9.3×10^{-12} m^2 s^{-1}) is in agreement with the value from ref. 22 of 9.4×10^{-12} m^2 s^{-1} and consistent with estimated limits of greater than 5×10^{-12} m^2 s^{-1} at 37 °C (derived from permeability coefficient values from ref. 27 and 28 combined with a limiting value of the membrane–donor partition coefficient from this work). D for caffeine in PDMS at 32 °C estimated here (1.6×10^{-12} m^2 s^{-1}) is reasonably consistent with values of 6 and 7×10^{-12} m^2 s^{-1} at 37 °C, derived from permeability coefficient values (from ref. 27 and 29 respectively) combined with a value of the membrane–donor partition coefficient from this work.

The extents and rate coefficients of all eight permeant–solvent–membrane systems are shown in Fig. 6 as plots of calculated *versus* measured values of $C_{rec,\infty}$ (upper plot) and k (lower plot). Based on exponential fits to plots of C_{rec} *versus* time (see Fig. 2), the *measured* values of $C_{rec,\infty}$ and k are reasonably accurate with estimated uncertainties of the order of 10% or less. Uncertainties in the *calculated* values of $C_{rec,\infty}$ and k are mainly determined by the relatively high uncertainties in the measured partition coefficients of Fig. 1 but also include uncertainties in the ancillary parameters such as the donor and receiver compartment volumes and the membrane thickness and area. The overall uncertainties in the calculated $C_{rec,\infty}$ and k values are estimated to be of the order of approximately 50%. Within these uncertainties, a single, fitted value of D for each permeant + membrane combination successfully captures the effects of changing the donor solvent from PBS to squalane. It can be seen from Fig. 6 that the theoretical model simultaneously describes both the equilibrium ($C_{rec,\infty}$) and kinetic aspects (k) of the permeation behaviour of the eight diverse experimental systems reasonably well.

Of the eight permeant–solvent–membrane systems, it can be seen that one (caffeine permeating through PDMS from a PBS donor) is very slow, one (caffeine permeating through cellulose from a squalane donor) is very fast and all other systems show similar "medium" rates. The key factor determining the observed differences in k over nearly 4 orders of magnitude are the relative values of the sum of the partition coefficients ($K_{mem-don} + K_{mem-rec}$). The differences in diffusion coefficient D between the different systems are of secondary importance in affecting k.

Discussion

The strategy adopted here of quantitatively analysing experimental permeation data in terms of a theoretical model based on clearly established underpinning assumptions provides a clear and systematic means of determining the origins of the many different possible ways in which the donor solvent might affect permeation. For systems for which the model assumptions are valid, the model shows that donor solvent effects on the extent and rate of membrane permeation are primarily controlled by how the three partition coefficients $K_{don-rec}$, $K_{mem-don}$ and $K_{mem-rec}$ change with donor solvent. The extent of permeation is determined by the relative volumes of the donor and receiver compartments and the value of $K_{don-rec}$. For equal donor and receiver volumes, the permeation rate coefficient is proportional to the sum ($K_{mem-don} + K_{mem-rec}$) and hence the magnitude of the donor

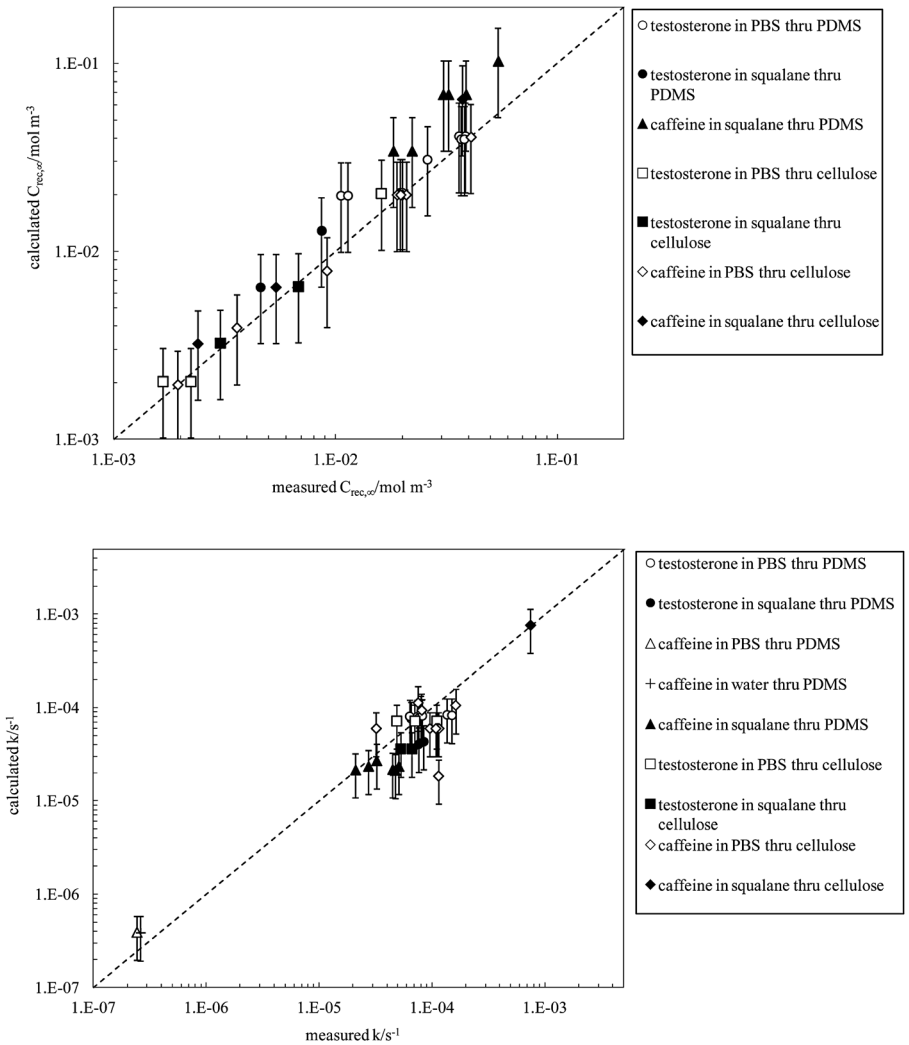

Fig. 6 Comparison of measured and calculated values of the equilibrium fraction of permeant extracted to the receiver compartment $C_{rec,\infty}$ (upper plot) and permeation rate constant k (lower plot) and for all the different combinations of permeant, donor solution solvent and membrane. The dashed lines indicate perfect agreement between theory and experiment.

solvent effect on rate is strongly affected by the natures of both the membrane and the permeant, as seen in Table 1.

For the experimental permeation cell used here (with stirring in both donor and receiver compartments), most of the permeation systems investigated follow the behaviour predicted by the model, *i.e.* the set of model assumptions are valid in most of the systems. Observed deviations from the model enable full and systematic discussion of all the additional possible ways in which the donor solvent can affect permeation, *i.e.* those effects not simply related to partition coefficient changes. The additional possible effects arise from solvent changes rendering one or more of the model assumptions invalid are therefore discussed under sub-headings which link to the key model assumptions.

1. The rate-limiting step changes from membrane diffusion

The first model assumption is that permeant diffusion across the membrane is rate-limiting and that all other mass transport and partitioning steps are relatively fast; this key assumption justifies the use of pseudo-equilibrium equations for the various partitioning processes. The model predicts the important "signature" features expected for permeation with rate-limiting membrane diffusion which are: (i) plots of C_{rec} *versus* time are exponential; (ii) the permeation rate coefficient k is independent of the initial permeant concentration and (iii) the permeation rate coefficient is independent of stirring speed (for stirring rates above a lower threshold). Fig. 4 and 5 show how the caffeine–squalane–cellulose system deviates from the model in these three aspects and is thereby revealed as having undergone a change in rate limiting step. In general, for the membrane thicknesses and membrane diffusion coefficients seen here, membrane diffusion is expected to remain rate-limiting when (i) donor and receiver compartments are stirred; (ii) the donor solvent viscosity is not too large and (iii) the membrane partition coefficients are such that very fast permeation is not obtained. The switch in rate-limiting step observed here for the caffeine–cellulose system when changing the donor solvent from PBS to squalane, is a result of the high viscosity of squalane relative to PBS plus the fact that the sum of the partition coefficients

($K_{mem-don}$ + $K_{mem-rec}$) favours very fast permeation for squalane as the donor solvent.

We note here that rate-limiting membrane diffusion is not desirable in particular applications which require slow or sustained drug release profiles. There is an extensive literature describing a wide range of different types of donor compartment formulations in which the drug or other active species is encapsulated using, for example, polymers within the donor vehicle.[30–32] Even for these formulations, it remains important to establish unambiguously that membrane diffusion is not rate-limiting under the particular experimental conditions used in order to correctly interpret permeation measurements.

2. Lag time is not negligibly small relative to the overall permeation time scale

The model predictions assume that the permeant concentration gradient across the membrane is linear, corresponding to "steady-state" diffusion, which is valid at times longer than the lag time. Hence, for the plots of C_{rec} *versus* time to exhibit the predicted exponential shape, it is required that the lag time L is negligibly small relative to the timescale of the overall permeation run. As seen in Table 2, the values of L estimated using eqn (15) and the fitted values of D for the different systems range from 24–683 s. Given that L is generally small relative to the permeation time scale of 5–50 hours, deviations from exponential shape in the overall plots of C_{rec} *versus* time are generally small, as seen, for example, in Fig. 2. However, the small deviations are observable by "zooming in" on the short time behaviour, particularly for the caffeine–PDMS systems where L is estimated to be relatively large. Fig. 7 shows two examples of the short time behaviour of plots of C_{rec} *versus* time. The testosterone–PBS–cellulose system (with estimated L of 24 s) is compared with the caffeine–squalane–PDMS system with estimated L of 683 s. For each plot, the dashed straight line indicates exponential behaviour seen for times $\gg L$. The solid lines correspond to fitted curves

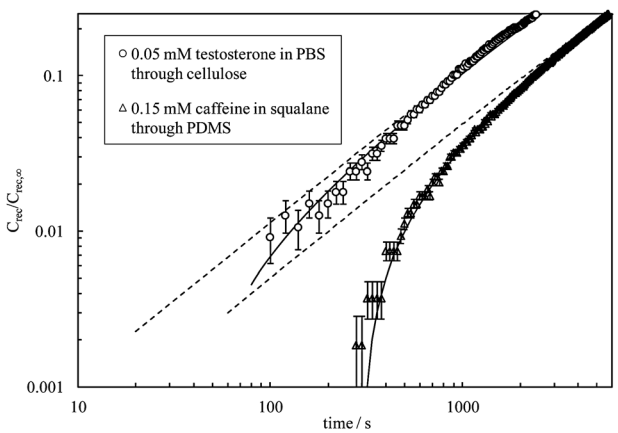

Fig. 7 Illustrative plots of the short-time behaviour of $C_{rec}/C_{rec,\infty}$ *versus* time for testosterone in PBS through cellulose (estimated L = 24 s) and caffeine in squalane through PDMS (estimated L = 683 s). For each plot the dashed line indicates exponential behaviour corresponding to L = 0. The solid dashed lines are fits to eqn (16) with the floated value of L = 40 and 300 s respectively, as described in the text.

which are reasonably well described using eqn (16) with floated values of L.

$$C_{rec} \approx C_{rec,\infty} + (C_{rec,0} - C_{rec,\infty}) \exp(-k\{t - L\}) \quad (16)$$

Qualitatively, it can be seen that the deviations from exponential behaviour are much greater for caffeine/squalane/PDMS than for testosterone/PBS/cellulose. Semi-quantitatively, fitting the curves of Fig. 7 to eqn (16) yields approximate values of L of 40 and 300 s respectively. Quantitative agreement with the L values from Table 2 (24 and 683 s respectively) is rather poor; this is probably due to the experimental uncertainty in the start time of the permeation runs which is estimated to be of the order of 2 minutes or so. In principle, measurement of the lag time provides a method to obtain an independent estimate of the diffusion coefficient D. As shown by the comparison of the different estimates of the lag time, this is unreliable for the experimental procedure used here.

Deviations from the predicted model behaviour due to lag time effects are expected for systems with thick membranes and low values of the diffusion coefficient (eqn (15)). In general, the effect is not dependent on the donor solvent. However, it is important to be aware of whether or not permeation runs are occurring under steady or non-steady state conditions in order to avoid incorrect interpretation of experimental permeation kinetic data.

3. Membrane diffusion follows Fick's laws and the membrane is uniform

In the derivation of the model equations, it is assumed that pseudo-equilibrium partitioning of the permeant occurs from the solvents to the membrane and that the membrane properties are uniform throughout its depth. For partitioning to occur, the membrane must be liquid-like rather than crystalline which will be the case for a synthetic polymer membrane at a temperature above its glass transition temperature. This is valid for PDMS but is almost certainly not the case for dry cellulose. However, as noted earlier, the cellulose membrane used here is pre-soaked in PBS and maintained in contact with a PBS receiving phase during permeation. The dry cellulose membrane swells to almost double its thickness following equilibration with PBS and so the actual membrane used consists of approximately 50% cellulose and 50% water. This water swollen membrane is likely to be liquid-like and thus the assumption made here is expected to be valid. The PDMS membrane properties are thought to be uniform throughout its depth. For the cellulose, we have noted that contact with PBS causes swelling in thickness but not in area and hence the membrane must possess anisotropic properties. However, there is no evidence that the membrane properties vary throughout the *depth* of the membrane (*i.e.* the direction of membrane permeation) and hence it is thought the assumptions made here are valid.

The model derived here will not be valid for composite membranes containing both liquid-like and solid regions for which the membrane properties will not be uniform throughout the membrane depth. This will be the case for synthetic membranes which have a degree of crystallinity, composite

membranes containing solid filler particles or for natural membranes such as the stratum corneum of skin which is a composite containing regions of lipid and corneocytes.[33] For such membranes, there will be additional considerations relating to, for example, the "tortuosity" of the permeant's pathway through the membrane. However, factors such as the tortuosity are not expected to be affected by the choice of donor solvent unless the solvent alters the membrane structure, *e.g.* the degree of crystallinity.

4. Donor and/or receiver solvents may permeate or affect the membrane

It is assumed in the model that only the permeant species permeates through the membrane and that its diffusion coefficient in the membrane is independent of its concentration in the membrane. Changing the donor solvent can affect permeation by rendering these assumptions invalid in several ways. Firstly, if the nature of the donor solvent is such that the permeant partitioning from donor to membrane is high, high permeant concentration in the donor compartment would give locally high permeant concentrations in the membrane which could affect the diffusion coefficient and cause it to depend on the localised (membrane depth dependent) permeant concentration. Such behaviour would result in non-exponential permeation plots. For the experimental systems measured here, this effect cannot be rigorously excluded but the lack of deviation from exponential curves due to this cause and the overall agreement between theory and experiment seen in Fig. 6 suggest that the effect, if present, is reasonably small.

Secondly, different donor solvents may swell the membrane to different extents and thereby affect the partitioning and diffusion coefficient of the permeant in the membrane. The effect has been reported in many literature studies of solvent effects in permeation[7–12] but is not present for the experimental systems studied here. As noted earlier, PDMS membranes show no significant swelling in either PBS or squalane solvents. The cellulose membranes are swollen in thickness (but not area) by PBS and not swollen by squalane. Because the cellulose membranes were pre-soaked in PBS and remained in contact with the PBS receiver solution during the permeation runs, the nature of the membrane was not affected by switching the donor solvent. For the cellulose membranes, the final values of all partition and diffusion coefficients listed in Table 2 refer to the PBS-saturated membrane rather than "dry" cellulose. Further evidence for the lack of this type of solvent effect arises from the observation that a single value of D successfully accounts for both PBS and squalane as donor solvent for all the membrane–permeant combinations (Table 2).

The third type of solvent effect which might invalidate this model assumption occurs when the donor and receiver solvents are mutually miscible to a significant extent and can permeate the membrane during a permeation run. In this case, the solvent compositions of both the donor and receiver compartment will change during a permeation run. Such time-dependent solvent compositions will cause time-dependent changes in the partition coefficients which, in turn, will cause deviations from the predicted exponential behaviour. This possibility can be excluded for the experimental systems measured here since aqueous PBS and squalane are not miscible to any significant extent. The effect has been observed in our laboratories for propylene glycol as donor solvent, PBS as receiver solvent, a cellulose membrane and either caffeine or testosterone as permeant. Large deviations from exponential behaviour are observed since the propylene glycol and PBS are mutually miscible and can permeate the cellulose membrane at rates which are comparable with that of the main permeating species.

5. Non-ideal behaviour of the permeant solutions

As noted above, the model derivation assumes that all partition coefficients (expressed as the ratio of equilibrium concentrations equal to the apparent value of K) are single-valued and independent of concentration. In fact, only the thermodynamic partition coefficient equal to the ratio of activities is a true constant; non-ideal solution behaviour can cause the apparent partition coefficient to be a function of permeant concentration, and hence time, during a permeation kinetic run. Because solution non-ideality depends on the balance of solvent–solvent, solvent–solute and solute–solute interactions, it should always be considered as a possible contribution to an observed, overall donor solvent effect in permeation. All solutions behave ideally in the limit of infinite dilution and hence activity coefficients are likely to progressively deviate from unity with increasing concentration which, in turn, may cause changes in the apparent K values at higher concentrations. If the concentration change during a permeation experiment causes a significant change in the apparent K value, then this alteration in K during the run is predicted to lead to deviations from the exponential form of the C_{rec} *versus* time plot. If the apparent K value is constant over the concentration range of the permeation run but was measured at a different concentration, then exponential behaviour is predicted but the measured apparent K value may not equal the value appropriate for the analysis of the permeation run. To avoid both types of potential error, it is recommended to measure the apparent K value as a function of concentration. Overlaying the concentration ranges of the permeation runs then enables proper selection of the apparent K value which is appropriate to the permeation run(s). The application of this approach to the experimental systems studied here is shown in Fig. 1. It can be seen there that the practice of estimating an apparent K value from the ratio of permeant solubilities in the two solvents is not recommended; the resultant apparent K value refers to the maximum accessible concentrations where non-ideality effects will, in general, be largest.

For the systems studied here, Fig. 1 shows that approximately constant apparent K values which are appropriate to the concentration ranges of the permeation runs can be selected for most systems. The exception is caffeine partitioning between PBS and a cellulose membrane where non-ideality effects are large over the relevant concentration range. In this case, the data of Fig. 1 was used to obtain different apparent K values which were approximately valid for the average concentration range of the different individual permeation runs with different initial permeant concentrations.

Conclusions

We have sought to establish a framework by which donor solvent effects and all their different possible origins can be resolved and understood. Based on well established and rigorous physico-chemical principles, we have developed an explicit set of equations to describe the equilibrium and kinetic behaviour of permeating systems for which a set of five key assumptions are valid. For such systems, the model predicts the key features of permeating systems obeying these assumptions and how their validity or otherwise can be experimentally tested. For systems which obey the model assumptions and conditions of constant permeation cell geometry and permeant diffusion coefficient within the membrane, the effects of changing the donor solvent on the extent and rate of membrane permeation are entirely determined by two equilibrium partition coefficients: $K_{mem–don}$ and $K_{mem–rec}$.

Additional possible donor solvent effects can arise when changing the donor solvent renders one or more of the key model assumptions invalid. Hence, in addition to altering permeation through changes in $K_{mem–don}$ and $K_{mem–rec}$, changing the donor solvent can:

(1) Alter the permeation rate-limiting step from membrane diffusion.

(2) Change whether or not the membrane diffusion occurs under steady-state conditions.

(3) Alter the membrane structure or uniformity.

(4) Cause time-dependent changes in the solvent composition of the membrane or the donor and receiver phases.

(5) Affect the extent of non-ideal permeant solution behaviour.

Using comparison of model predictions and experimental data for eight permeation systems which differ widely in the hydrophobicity/hydrophilicity of the permeant, donor solvent and membrane, we have been able to identify and quantify effects including a change in the rate-determining step of permeation, non-ideal solution behaviour of the permeant solutions and deviations due to non-steady-state conditions. Overall, the main outcome of this study is the development of a rigorous theoretical and experimental framework whereby donor solvent effects in permeation can be determined and their origins fully elucidated.

Abbreviations

PBS	phosphate buffered saline solution in water
PDMS	polydimethylsiloxane

Glossary of terms

V_{rec}	volume of receiving compartment
V_{don}	volume of donor compartment
C_{don}	concentration of permeating species in the donor compartment
C_{rec}	concentration of permeating species in the receiving compartment
$C_{mem,d}$	local concentration of permeating species in the membrane at the interface with the donor compartment
$C_{mem,r}$	local concentration of permeating species in the membrane at the interface with the receiving compartment
$K_{rec–mem}$	equilibrium partition coefficient of the permeating species between the receiving phase and the membrane ($=C_{rec}/C_{mem,r}$)
A	surface area of membrane
n_t	total number of moles of permeating species
x	distance co-ordinate within the membrane (perpendicular to its surface)
X	total thickness of the membrane
D	diffusion coefficient of the permeating species within the membrane
k	1st-order permeation rate coefficient
L	time taken to establish the steady-state concentration gradient of permeant across the membrane (“lag time”)

Acknowledgements

We thank the Engineering and Physical Sciences Research Council (EPSRC, UK) and GSK, Barnard Castle, UK for an Industrial CASE Award and Dow Corning, Europe SA for the PDMS membranes.

References

1 A. C. Watkinson, H. Joubin, D. M. Green, K. R. Brain and J. Hadgraft, *Int. J. Pharm.*, 1995, **121**, 27.
2 S. E. Cross, W. J. Pugh, J. Hadgraft and M. S. Roberts, *Pharm. Res.*, 2001, **18**, 999.
3 P. C. Mills, *Vet. Res. Commun.*, 2007, **31**, 227.
4 M. Dias, J. Hadgraft and M. E. Lane, *Int. J. Pharm.*, 2007, **340**, 65.
5 M. Dias, J. Hadgraft and M. E. Lane, *Int. J. Pharm.*, 2007, **336**, 108.
6 A. Fini, V. Bergamante, G. C. Ceschel, C. Ronchi and C. A. F. De Moraes, *AAPS PharmSciTech*, 2008, **9**, 762.
7 M.-L. Leichtnam, H. Rolland, P. Wuthrich and R. H. Guy, *J. Controlled Release*, 2006, **113**, 57.
8 W. J. McAuley, K. T. Mader, J. Tetteh, M. E. Lane and J. Hadgraft, *Eur. J. Pharm. Sci.*, 2009, **38**, 378.
9 W. J. McAuley, M. D. Lad, K. T. Mader, P. Santos, J. Tetteh, S. G. Kazarian, J. Hadgraft and M. E. Lane, *Eur. J. Pharm. Biopharm.*, 2010, **74**, 413.
10 G. Oliveira, A. E. Beezer, J. Hadgraft and M. E. Lane, *Int. J. Pharm.*, 2010, **393**, 61.
11 W. J. McAuley, G. Oliveira, D. Mohammed, A. E. Beezer, J. Hadgraft and M. E. Lane, *Int. J. Pharm.*, 2010, **396**, 134.
12 R. M. Watkinson, R. H. Guy, G. Oliveira, J. Hadgraft and M. E. Lane, *Skin Pharmacol. Physiol.*, 2011, **24**, 22.
13 P. Izquierdo, J. W. Wiechers, E. Escribano, M. J. Garcia-Celma, T. F. Tadros, J. Esquena, J. C. Dederen and C. Solans, *Skin Pharmacol. Physiol.*, 2007, **20**, 263.
14 K. Wiren, H. Frithiof, C. Sjoqvist and M. Loden, *Br. J. Dermatol.*, 2009, **160**, 552.
15 A. Otto, J. du Plessis and J. W. Wiechers, *Int. J. Cosmet. Sci.*, 2009, **31**, 1.
16 S. Simovic and C. A. Prestidge, *Eur. J. Pharm. Biopharm.*, 2007, **67**, 39.
17 H. Sarhan, M. A. Ibrahim, M. A. Amin and A. K. F. Dyab, *Bull. Pharm. Sci., Assiut Univ.*, 2008, **31**, 155.
18 J. Frelichowska, M. A. Bolzinger, J. Pelletier, J. P. Valour and Y. Chevalier, *Int. J. Pharm.*, 2009, **371**, 56.
19 J. Frelichowska, M. A. Bolzinger, J. P. Valour, H. Mouaziz, J. Pelletier and Y. Chevalier, *Int. J. Pharm.*, 2009, **368**, 7.
20 N. G. Eskandar, S. Simovic and C. A. Prestidge, *J. Pharm. Sci.*, 2010, **99**, 890.
21 S. Simovic, N. G. Eskander and C. A. Prestidge, *J. Drug Delivery Sci. Technol.*, 2011, **21**, 123.

22 B. P. Binks, P. D. I. Fletcher, A. J. Johnson and R. P. Elliott, *Langmuir*, 2012, **28**, 2510.
23 S. H. Yalkowsky and Y. He, *Handbook of Aqueous Solubility Data*, CRC Press, Boca Raton, 2003.
24 H. L. Frisch, *J. Phys. Chem.*, 1958, **62**, 401.
25 A. Kumagai and S. Takahashi, *Int. J. Thermophys.*, 1995, **16**, 773.
26 *Thermodynamics Research Center AP144 Hydrocarbon Project. Selected values of properties of hydrocarbons and related compounds*, Texas A&M University, Thermodynamics Research Center, 1978.
27 G. M. Khan, Y. Frum, O. Sarheed, G. M. Eccleston and V. M. Meidan, *Int. J. Pharm.*, 2005, **303**, 81.
28 Y. Frum, G. M. Eccleston and V. M. Meidan, *Eur. J. Pharm. Biopharm.*, 2007, **67**, 434.
29 M. Dias, A. Farinha, E. Faustino, J. Hadgraft, J. Pais and C. Toscano, *Int. J. Pharm.*, 1999, **182**, 41.
30 J. C. Moreau, B. Leclerc, J. Mazan, G. Couarraze, G. Torres and H. Porte, *J. Mater. Sci. Mater. Med.*, 1991, **2**, 243.
31 J. Siepmann, F. Lecomte and R. Bodmeier, *J. Controlled Release*, 1999, **60**, 379.
32 G. Piel, M. Piette, V. Barillaro, D. Castagne, B. Evrard and L. Delattre, *Int. J. Pharm.*, 2006, **312**, 75.
33 See, for example J. Hadgraft, *Eur. J. Pharm. Biopharm.*, 2004, **58**, 291.

